J Solid State Electrochem (2006) 10: 416–421
DOI 10.1007/s10008-005-0012-z

ORIGINAL PAPER

C. Sunseri · C. Spadaro · S. Piazza · M. Volpe
F. Di Quarto

Porosity of anodic alumina membranes from electrochemical measurements

Received: 15 February 2005 / Accepted: 11 May 2005 / Published online: 20 July 2005

Abstract A procedure based on the high-field mechanism of the growth of anodic oxides was developed in order to evaluate the morphological features of porous layers. Since the thickness of the barrier film, separating the porous layer from the metal, does not change during the steady-state growth of an anodic porous layer, the rate of displacement of the metal-oxide interface to the metal direction must be equal to the rate of displacement of the pore base to the oxide direction. As a consequence, porosity can be expressed in terms of the ratio i_{diss}/i_{ion}, where i_{diss} is the dissolution current density at the pore base, and i_{ion} is the ionic current density at the metal-oxide interface. Pore diameter can be determined from geometrical considerations, while average pore population can be obtained from the ratio of porosity to the average surface area of a single pore. This procedure was checked by comparison with experimental results relative to membranes prepared in various conditions. The satisfactory agreement between theoretical and experimental findings indicates that porosity can be evaluated by current density data and vice-versa. Therefore, anodic alumina membranes may be tailored for different applications by choosing operative conditions giving the desired value of i_{diss}/i_{ion}.

Keywords Alumina membrane · Porosity · Aluminium anodising

Introduction

In the past, the aluminium anodising process forming alumina porous layers was widely investigated for the fabrication of protective, corrosion-resistant coatings [1]. Recently, attention has been focused again on this process for the fabrication of anodic alumina membranes [2, 3] which can be obtained from anodic porous layers, after dissolving the remaining metal and oxide barrier film separating metal from the pore bottom. The interest in this type of membrane is due to its morphological characteristics and to its chemical and thermal stability, allowing it to be used in aggressive environments where the most common polymeric membranes do not resist. Specifically, anodic alumina membranes contain cylindrical pores perpendicular to the surface. Each pore is at the centre of hexagonal cells distributed on the surface to form a highly ordered two-dimensional array. For this reason, these membranes were studied in order to be used as host or nano-structured templates for magnetic, electronic and optoelectronic devices [4]. Other possible applications are in the field of catalysis, where they can be used as a catalyst support, and for the fabrication of catalytic membrane reactors [5].

A relevant issue is the possibility to easily control the morphological characteristics of anodic alumina membranes by changing the anodising conditions. A key parameter is the solvent action of the electrolyte, but it is also necessary to take into account voltage, anodising time, bath temperature, the detachment procedure of porous layers, and final treatments of membranes. Moreover, depending on the end use of the membranes, different initial treatments may be necessary [6]. Highly ordered structures can be obtained, either by anodising at a voltage leading to a moderate expansion of the aluminium oxide during aluminium oxidation [7] or by anodising textured aluminium surfaces obtained by molding [8]. On the contrary, there are less constraints in the preparation procedure of membranes if they are to be used in the field of catalysis, because, for this application, the order of the structure is less important.

Some of these issues have been investigated in previous works, dealing with the preparation of anodic alumina membranes in different conditions [9, 10]. These works highlighted the necessity to investigate the growth process

C. Sunseri (✉) · C. Spadaro · S. Piazza
M. Volpe · F. Di Quarto
Dipartimento di Ingegneria Chimica dei Processi e dei Materiali,
Università di Palermo, Viale delle Scienze,
90128, Palermo, Italy
E-mail: sunseri@dicpm.unipa.it
Tel.: +39-91-6567231
Fax: +39-91-6567280

of porous layers in order to determine measurable parameters strictly related to the morphological features of membranes. In this study, we report some results relative to this issue. On the basis of the most common mechanism of pore initiation and growth on aluminium reported in the literature [11–13], we developed a simple model to evaluate the morphological characteristics of membranes by electrochemical measurements. The results of the model closely correspond to the experimental findings, so that it was possible to demonstrate that the porosity of alumina anodic membranes closely depends on the relative rate of ejection and/or field assisted dissolution of aluminium ions at the pore bottom to oxidation rate of metal. On the basis of the previous cited anodising mechanism adopted in this work to calculate the porosity of the membrane, both anion and cation transport numbers can be determined by evaluating the partition of the total current density (c.d.).

Experimental

Anodic alumina layers were obtained by the electrochemical oxidation of aluminium (99.99% purity). Circular electrodes (diameter: 3.2 cm) were cut from 100 μm thick aluminium foils, cleaned by immersion in 1 M NaOH for 3 min, and washed in distilled water. Discs were electrochemically polished at 20 V for 5 min in a vigorously stirred HClO4:C2H5OH solution (1:6 by volume) and washed once more in sonicated distilled water. Finally, electrodes were mounted on a holder in order to have a flat circular surface exposed to the solution. Anodisations were performed by linear potential sweep at 0.2 V s^{-1} up to 70 V in 0.15 M oxalic acid and 20 V in 1.5 M H_2SO_4. Then the cell voltage was held constant in order to grow porous layers of the desired thickness. After an initial fast transient due to the switch from potential linear scan to tensiostatic polarisation, the c.d. reached almost constant values. A Glassman High Tension (series ER) power source and a two-electrode cell, having a Pt wire as the counter electrode, were used. The temperature of the anodising bath was controlled within ± 0.1°C by means of a Lauda refrigerator (mod RE 106). During anodising the electrolyte was stirred vigorously.

The morphology of the samples was examined at different magnifications with a Philips XL30ESEM scanning electron microscope (SEM). Prior to SEM examination, the oxide surfaces were sputter coated with gold. In order to observe the pore arrangement at the metal-oxide interface, the aluminium substrate was totally dissolved in 0.1 M CuCl + 20% (w/w) HCl solution at 5°C; then the pore bottoms were opened by chemical etching in 1 M phosphoric acid solution at 35°C. In order to expose only the barrier layer side to the solution, the porous layer was mounted onto a holder.

In order to evaluate by Faraday's law the different contributions to the total current, i, measured during aluminium anodising, gravimetric measurements were conducted. The weight of the aluminium discs was measured before anodising. After anodising, samples were thoroughly rinsed with distilled water and then with acetone, in order to remove the water completely. After drying in an oven at 60°C for 3 h, samples were weighed again. The amount of residual aluminium was evaluated by the difference between the weight of the anodised sample and the weight of the porous layer after dissolution of the metal in CuCl solution. Taking into account the possibility that this step could cause fatal errors, a very accurate procedure was followed. Porous layers were rinsed first with water and after with acetone, then dried overnight in an oven at 100°C before weighing. In order to exclude the possible modification of porous layers during the immersion into the CuCl solution, we tested this treatment on a commercial membrane (Whatman, U.K.). We found that the weight of the commercial membrane did not change after immersion in the CuCl solution. Moreover, elemental analysis by energy dispersive spectroscopy, EDS (Philips mod. PV7760), performed on both commercial membranes and porous layers after CuCl treatment did not reveal the presence of Cl.

Results and discussion

The c.d. measured during the growth of a porous layer, i, was the sum of the ionic c.d., i_{ion}, which was the oxidation current of the aluminium at the metal/oxide interface, and electronic c.d., i_{el}, due to faradaic processes occurring at the oxide/electrolyte interface, such as oxygen evolution. Moreover, i_{ion} was the sum of the formation current density, i_{form}, indicating the c.d. contribution to forming new oxide, and the dissolution current density, i_{diss}, related to the field-assisted dissolution of Al^{3+} ions into the electrolyte at the pore bottom. As a consequence, we can write

$$i = i_{ion} + i_{el} = i_{form} + i_{diss} + i_{el} \tag{1}$$

By weight measurements and applying Faraday's law, it was possible to evaluate each term of Eq. 1 [9]. The average i_{ion} and i_{form} were evaluated as follows:

$$(i_{ion})_{av} = \frac{1}{S_m}\frac{(\Delta m)_{Al}}{(M_w)_{Al}}\frac{zF}{\Delta t} \tag{2}$$

$$(i_{form})_{av} = \frac{1}{S_m}\frac{m_{form}}{(M_w)_{Al_2O_3}}\frac{zF}{\Delta t} \tag{3}$$

where S_m is the apparent surface area of the sample, $(\Delta m)_{Al}$ is the amount of aluminium consumed during anodising, m_{form} the weight of the porous layer, $(M_w)_{Al}$ and $(M_W)_{Al_2O_3}$ the molecular weight of Al and Al_2O_3, respectively. From Eqs. 1, 2, 3 the average dissolution current can be calculated as

$$(i_{diss})_{av} = (i_{ion})_{av} - (i_{form})_{av} \tag{4}$$

Typical features of a membrane are porosity, average pore size, pore population and length of the channels. In the case of anodic alumina membranes, the channels are cylindrical and perpendicular to the surface; therefore, their length is equal to the thickness of the membrane. As a consequence, porosity, usually given by the ratio of pore volume to total volume, is almost equal to:

$$P = S_p/S_m \tag{5}$$

where S_p is the total surface of pores and S_m is the geometrical area of the membrane. The validity of this equation rests on the assumption that pore diameter is uniform along the whole thickness of porous layers; therefore pore mouth enlargement due to chemical dissolution of alumina should be negligible. This assumption is supported by the plots of Fig. 1 showing a linear dependence of the thickness on the passed charge for membranes formed in oxalic acid solutions at 70 V and different temperatures, and in sulphuric acid solutions at 20 V and 16°C. The linearity rules out significant effects of chemical dissolution at the pore mouths, otherwise a bend of the plots to the right should be observed [14].

According to the high field theory of growth of anodic films, i_{ion} is related to the electric field strength [15, 16].

Since the potential drop across the barrier film can be assumed to be practically coincident with the applied voltage, we can conclude that under steady-state conditions the thickness of the barrier film must be constant.

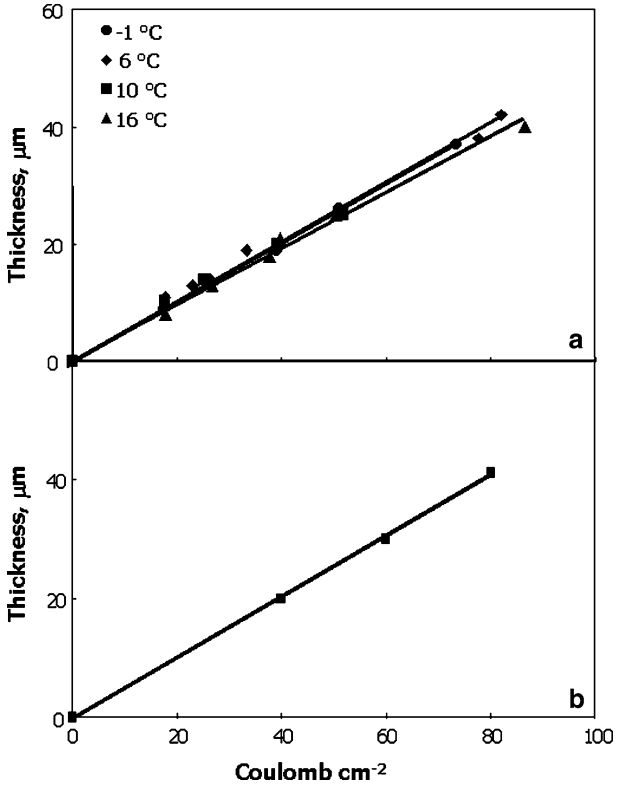

Fig. 1 Thickness versus electric charge for porous layers grown in **a** 0.15 M oxalic acid solution at at different temperatures and 70 V; **b** 1.5 M H_2SO_4 solution at 16°C and 20 V

The growth of a porous layer is accompanied by volume changes simultaneously occurring at both metal/oxide and barrier layer oxide/electrolyte interfaces. The volume change at the metal/oxide interface is due to the metal oxidation generating Al^{3+} ions, while the other volume change is due to Al^{3+} ions ejection and/or field assisted dissolution occurring at the pore bottom. Taking a mass balance about the barrier film with t^+ and t^- transport number of cation and anion respectively, t^- Al^{3+} ions react at the metal/oxide interface with O^{2-} ions injected at the barrier layer oxide/electrolyte interface to form fresh oxide, while t^+ Al^{3+} ions, migrating from the metal, dissolve into the electrolyte because at the pore bottom no oxide formation occurs [11–13]. This mechanism implies that a fraction of the metal volume oxidised at the metal/oxide interface is lost at the barrier layer/electrolyte interface.

If the barrier layer thickness does not change during the steady-state formation of a porous layer, the rate of the displacement of the metal/oxide interface toward the metal (Δl), must be equal to the rate of displacement of the pore bottom toward the oxide ($\Delta l'$). The displacement rates per unit time of both metal and pore bottom respectively are

$$\Delta l = \Delta V_{M-ox}/S_m \quad \Delta l' = \Delta V_{M-elettr}/S_p \tag{6}$$

where $\Delta V_{M\text{-}ox}$ is the rate per unit time of volume change accompanying metal oxidation, while $\Delta V_{M\text{-}elettr}$ is the rate per unit time of volume change due to metal loss in the electrolyte.

By applying Faraday's law, we have

$$\Delta V_{M-ox} = \frac{i_{ion}}{(zF\rho_{Al})} \quad \Delta V_{M-elettr} = \frac{i_{diss}}{(zF\rho_{Al})} \tag{7}$$

where F is Faraday's constant, and ρ_{Al} the molar density of aluminium.

Since Δl and $\Delta l'$ in Eq. (6) must be equal, we can write

$$P = \frac{S_p}{S_m} = \frac{\Delta V_{M-elettr}}{\Delta V_{M-ox}} = \frac{i_{diss}}{i_{ion}} \tag{8}$$

If D is the diameter of the circle inscribed within an hexagonal cell, the pore diameter is

$$\phi = D - 2s \tag{9}$$

with s the thickness of the pore wall. Pore population, N_p, is related to the pore diameter by the relationship

$$N_P = \frac{S_p}{(\pi\phi^2/4)} \tag{10}$$

Porosity can also be expressed according to

$$\frac{S_p}{S_m} = \frac{N_p\pi\phi^2/4}{N_p A_{hex}} \tag{11}$$

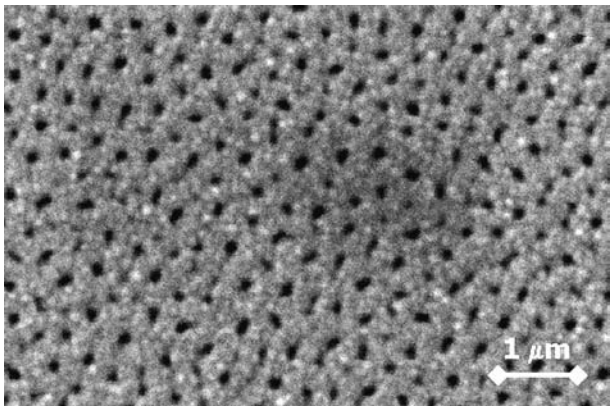

Fig. 2 SEM picture showing the morphology of a porous layer grown in 0.15 M oxalic acid solution at 16°C and 70 V

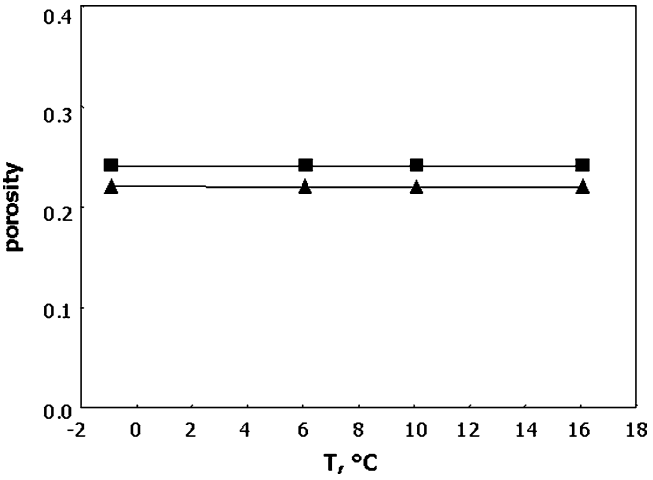

Fig. 3 Porosity of layers anodically grown on aluminium in 0.15 M oxalic acid at different temperatures. • SEM analysis; • Eqs. 7, 8, 9, 10 and 11, 12

Where A_{hex} is the area of a regular hexagon circumscribing a circle with a diameter D. On the basis of geometrical considerations, we have $A_{hex} = 2.60*L^2$ (L = side length of hexagon) and $D/2 = 0.8660*L$, from which we obtain $A_{hex} = 3.467*D^2/4$.

From Eqs. 9 and 11, we obtain

$$\phi = \frac{2sP^{0.5}}{(0.952 - P^{0.5})} \tag{12}$$

We can determine porosity by Eq. 8 while pore diameter and pore population can be evaluated by Eqs. 12 and 10, respectively, with s an adjustable parameter determined by the best fit with the experimental data.

The reliability of the model was checked by comparison with experimental results obtained in different conditions. In particular, the morphological parameters of membranes formed in oxalic acid at different temperatures and in 1.5 M H_2SO_4 at 16°C were considered.

Figure 2 shows a SEM picture of a porous layer formed in 0.15 M oxalic acid solutions at 16°C and 70 V. Similar morphologies were observed at lower temperatures.

Table 1 shows the results of gravimetric measurements and the values of ionic, formation and dissolution c.ds. evaluated in 0.15 M oxalic acid at 70 V and different anodising temperatures. In the same conditions, the porosity values determined by SEM were found to change from 26.9 % to 22 % [9]. The average value of 24 % closely agrees with the porosity value of 22 % calculated by Eq. 8 as shown in Fig. 3. In the same work [9] it has been shown that the pore size of membranes changed from 90.4 nm at −1°C to 87.4 nm at 16°C. Since these values are very close, a mean value of 89 nm was assumed as a typical pore diameter. This experimental value is coincident with the average value of 90 nm calculated by Eq. (12) as shown in Fig. 4.

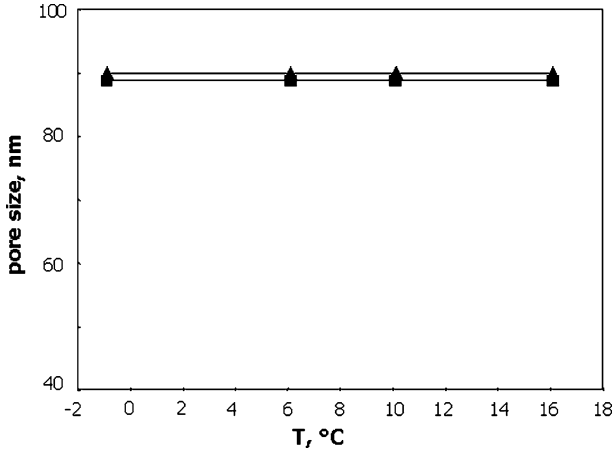

Fig. 4 Pore size of layers anodically grown on aluminium in 0.15 M oxalic acid at different temperatures. • SEM analysis; • Eqs. 7, 8, 9, 10 and 11, 12

Table 1 Gravimetric results to determine ionic (i_{ion}), formation (i_{form}) and dissolution (i_{diss}) c.ds. as function of the temperature for porous layers grown in 0.15 M oxalic acid at 70 V. (z thickness of porous layers; w_i initial weight of aluminium; w_f weight of samples at the end of the anodisation; w_m weight of porous layers; w_{ac} weight of aluminium consumed during anodisation;)

T (°C)	z (μm)	w_i (g)	w_f (g)	w_m (g)	w_{ac} (g)	i_{ion} (mA cm^{-2})	i_{form} (mA cm^{-2})	i_{diss} (mA cm^{-2})
−1	26	0.6588	0.6907	0.0994	0.0676	2.24	1.75	0.49
6	26	0.6089	0.6403	0.0979	0.0665	3.63	2.62	0.74
10	25	0.6111	0.6434	0.1006	0.0683	4.48	3.50	0.99
16	24	0.6348	0.6662	0.0978	0.0664	5.88	4.58	1.29

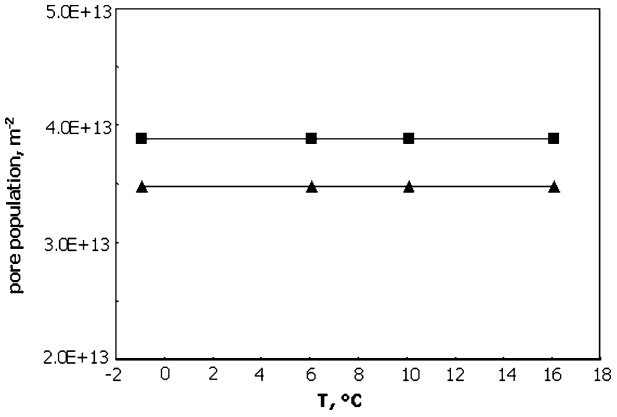

Fig. 5 Pore population of layers anodically grown on aluminium in 0.15 M oxalic acid at different temperatures. • SEM analysis; • Eqs. 7, 8, 9, 10 and 11, 12

Analogously, Fig. 5 shows that the average pore population of 3.48×10^{13} m^{-2}, calculated by Eq. (10), was very close to the average value of 3.88×10^{13} m^{-2} estimated by SEM analysis. The best fit with the experimental findings was found using $s=46$ nm in Eq. (9). On the basis of these results, it is possible to account for the independence from temperature of the morphological features of porous layers grown in oxalic acid, observed in a previous work [9]. This behaviour is attributable to the fact that when the temperature was increased from −1°C to 16°C, the relative increase of i_{ion} and i_{diss} was the same, so that the porosity did not change. As a consequence, also the other morphological parameters did not change, being related to porosity values.

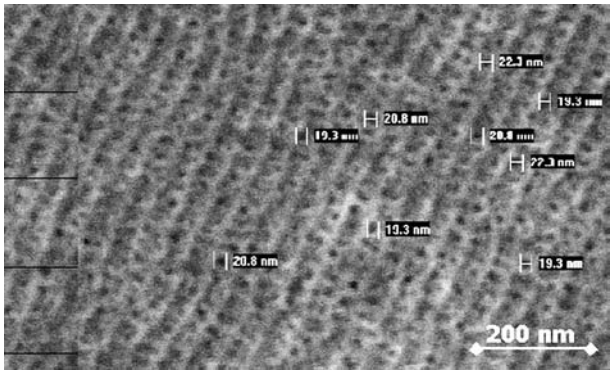

Fig. 6 SEM picture showing the morphology of a porous layer grown in 1.5 M H_2SO_4 solution at 16°C and 20 V

Figure 6 shows a SEM picture of a porous layer formed in 1.5 M H_2SO_4 at 16°C and 20 V. We can observe that in these conditions small circular pores, uniformly distributed over the surface, were formed. Table 2 shows the results of the gravimetric measurements and the calculated values of ionic, formation and dissolution c.ds. for the same samples. The typical morphological parameters of such a porous layer, estimated after averaging 10 different images, are summarised in Table 3, where the values calculated by Eqs. 8, 10, 12 are also cited. The values of both ionic and dissolution c.ds. were 20.17 and 3.53 mA cm^{-2} respectively. Table 3 confirms an excellent agreement between calculated and measured values in this case as well. The value of s used in Eq. 9 in order to obtain the best fit was 14.0 nm.

A further confirmation of the reliability of the model proposed here was obtained by the values of the pore wall thickness that was determined by the best fitting of experimental results. Some authors reported that the thickness of pore walls is equal to that of the barrier film [17] independently of the anodising electrolyte, while for anodising in 0.4 M H_3PO_4, a ratio of pore wall thickness to barrier layer thickness equal to 0.71 is reported [11]. Using the latter value for a porous layer grown in 1.5 M H_2SO_4 at 16°C, a unit barrier thickness of 0.99 nmV^{-1} was obtained that is coincident with 1 nm V^{-1} reported in the literature [18] for very similar conditions (15% H_2SO_4 at 10°C). Moreover, the cell size value of 48 nm calculated in the present work for a porous layer grown in 1.5 M H_2SO_4 at 16°C closely agrees with the value of 45 nm reported by the same authors.

For porous layers grown in 0.15 M oxalic acid solutions at different temperatures from −1°C to 16°C, the previous cited value of 0.71 cannot be used because, starting from the value of the pore wall thickness, evaluated here as an adjustable fitting parameter (46 nm), we obtain a unit barrier thickness lower than the 1.18 nm V^{-1} reported in the literature for porous layers grown in 2% oxalic acid at 25°C [18]. This discrepancy is not justifiable because the anodising ratio increases when both solution concentration increases and the temperature decreases [11], therefore, for the conditions of this study (lower temperature and slightly higher electrolyte concentration), we would expect a value of anodising ratio not below 1.18 nm V^{-1} . This finding suggests that the ratio of pore wall thickness to barrier layer thickness is the same for porous layers grown in both 0.4 M H_3PO_4 at 25°C and in 1.5 M H_2SO_4 solutions at 16°C while it is different for porous

Table 2 Gravimetric results to determine ionic (i_{ion}), formation (i_{form}) and dissolution (i_{diss}) c.ds. for porous layers grown at 16°C in 1.5 M H_2SO_4 20 V. (z thickness of porous layers; w_i initial weight of aluminium; w_f weight of samples at the end of the anodisation; w_m weight of porous layers; w_{ac} weight of aluminium consumed during anodisation;)

T (°C)	z (μm)	w_i (g)	w_f (g)	w_m (g)	w_{ac} (g)	i_{ion} (mA cm^{-2})	i_{form} (mA cm^{-2})	i_{diss} (mA cm^{-2})
16	30	0.3463	0.3731	0.0749	0.0481	20.17	16.64	3.53

Table 3 Morphological parameters obtained by both SEM analysis and electrochemical measurements of anodic porous layer formed in 1.5 M H_2SO_4, $T = 16°C$, and 20 V

	SEM	Electrochem
Pore size (nm)	20.4	20.1
Pore population (m^{-2})	5.61 E + 14	5.49 E + 14
Porosity (%)	18.5	17.5

layers grown in 0.15 M oxalic acid solutions at different temperatures from −1°C to 16°C. Therefore, we can hypothesise that this ratio depends on the nature of an electrolyte. Further investigations are necessary in order to better explain this issue.

The reliability of the model indirectly confirms the validity of the adopted mechanism of the growth of porous layers by aluminium anodising. This implies that the porosity value from Eq. 8 is coincident with the cation transport number. Since the anion transport number is given by the ratio i_{form}/i_{ion} in the absence of oxide formation at the electrolyte interface, we can conclude that starting from electrochemical measurements it is possible to evaluate the morphological parameters of the porous layers, and, vice-versa, starting from both porosity and i_{ion} values it is possible to evaluate both cation and anion transport numbers and current efficiency (referred to passing current density) for the formation of anodic alumina membranes.

The proposed model clearly confirms that morphological features of porous layers on aluminium depend on the ratio of Al^{3+} dissolution rate to Al^{3+} generation rate rather than on the solvent action of an electrolyte only.

Conclusions

The morphological features of porous layers electrochemically grown on aluminium were evaluated by a model developed on the basis of a possible mechanism of growth of these porous layers. Assuming that the thickness of barrier film remained unchanged when a porous layer was growing under steady-state conditions, porosity values were determined by the ratio of dissolution c.d. to ionic one, while the pore diameter was obtained by geometrical consideration correlating pore wall thickness to cell size. The model was validated by comparison with the experimental findings relative to porous layers formed in 0.15 M oxalic acid solutions at different temperatures and in 1.5 M sulphuric acid solutions at 16°C. The results of this comparison were highly satisfactory so that the model may help to tailor porous anodic alumina membranes by better choosing the operative conditions of aluminium anodising.

Acknowledgements The authors gratefully acknowledge financial support from MIUR – Cofin 2002.

References

1. Henley VF (1982) Anodic oxidation of aluminium and its alloys. Pergamon, Oxford
2. Furneaux RC, Rigby WR, Davidson AP (1989) Nature 337:147
3. Asoh H, Nishio K, Nakao M, Tamamura T, Masuda H (2001) J Electrochem Soc 148:B152
4. Kovtyukhova NI, Mallouk TE, Mayer TS (2003) Adv Mater 15:780
5. Julbe A, Farrusseng D, Guizard C (2001) J Membr Sci 181:3
6. Bocchetta P, Sunseri C, Masi R, Piazza S, Di Quarto F (2003) Mater Sci Eng C 23:1021
7. Jessennsky O, Müller F, Gösele U (1998) Appl Phys Lett 72:1173
8. Masuda H, Yamada Y, Satoh M, Asoh H, Naka M, Tamamura T (1997) Appl Phys Lett 71:2770
9. Bocchetta P, Sunseri C, Bottino A, Capannelli G, Chiavarotti G, Piazza S, Di Quarto F (2002) J Appl Electrochem 32:977
10. Bocchetta P, Sunseri C, Chiavarotti G, Di Quarto F (2003) Electrochim Acta 48:3175
11. O'Sullivan JP, Wood GC (1970) Proc Roy Soc Lond A 317:511
12. Siejka J, Ortega C (1977) J Electrochem Soc 124:883
13. Shimizu K, Kobayashi K, Thompson GE, Wood GC (1992) Phil Mag 66:643
14. Patermarakis G (1996) J Electroanal Chem 404:69
15. Bernard WJ, Cook JW (1959) J Electrochem Soc 106:643
16. Harkness AC, Young L (1966) Can J Chem 44:2409
17. Wehrspohn RB, Nielsch K, Birner A, Schilling J, Muller F, Li A-P, Gosele U (2001) Electrochemically prepared high-aspect ratio highly ordered pore arrays and applications. In: Schmuki P, Lockwood DJ, Ogata YH, Isaacs HS (eds) Pits and pores II: formation properties, and significance for advanced materials, vol 2000–25, The Electrochemical Society, Inc., Pennington, NJ, pp 168–175
18. Wernick S, Pinner R, Sheasby PG (1987) The surface treatment and finishing of aluminium and its alloys, 5th edn, vol 1 ASM International, Finishing Publications LTD. Teddington, Middlesex, England